Case Studies in Thermal Engineering 13 (2019) 100388

Contents lists available at ScienceDirect

Case Studies in Thermal Engineering

journal homepage: www.elsevier.com/locate/csite

Numerical investigation of heat transfer enhancement in plate-fin heat sinks: Effect of flow direction and fillet profile

Ammar A. Hussain[a], Basim Freegah[a], Basima Salman Khalaf[a], Hossein Towsyfyan[b,*]

[a] Mechanical Engineering Department, Mustansiriyah University, Baghdad, Iraq
[b] Institute of Sound and Vibration Research (ISVR), University of Southampton, UK

ARTICLE INFO

Keywords:
Computational fluid dynamic (CFD)
Heat sink
Fin
Thermal performance

ABSTRACT

Many researchers have studied the thermal performance of heat sinks, however to the best knowledge of the authors, the effect of flow direction (place of fan) on the thermal performance of plate-fin heat sinks with fillet profile have not yet been investigated. In this paper, the investigation develops a computational fluid dynamics (CFD) model, validated through comparison with an experimental data from the literature, which demonstrates the effect of flow direction and fillet profile on the thermal performance of plate-fin heat sinks. In particular, a plate-fin heat sink with fillet profile subject to parallel flow has been compared with the conventional design (plate-fin heat sink without fillet profile subject to an impinging flow) and satisfactory results have been perceived. The results of this study show that the base temperature along with the thermal resistance of the heat sink is lower for the proposed design. Therefore, the developed approach has strong potential to be used to improve the thermal performance of heat sinks and hence to develop more advanced effective cooling technologies.

1. Introduction

Power density in electronic and microelectronic equipment is significantly increasing due to recent advances in semiconductor technology. Therefore, in a highly competitive electronic equipment industry, the improvement of heat transfer rate for such devices is critically essential for long-term reliable operation.

Cooling the electronic devices by natural convection with the help of finned heat sinks is a common practice in industry due to several advantages (e.g. easy fabrication, powerless operation and high reliability). Heat sinks coupled with peripherals such as jets and fans are continuously developing to meet the requirement of higher heat dissipation [1].

Two common configuration of heat sinks are the parallel arrangement either of the rectangular cross section plate fins or with pin fins on a flat base. The former known as plate-fin heat sinks and the latter called pin-fin heat sinks.

Several studies demonstrate that attempts have been made to compare the efficiency of these configurations. For instance, F. Forghan et al. [2] reported that the thermal performance is considerably lower in plate-fin heat sinks compared to pin-fin heat sinks for the low air velocities. Contrary to this, research has been developed demonstrating that under certain conditions the thermal performance of the pin-fin heat sink is superior to that of the plate-fin heat sink [3,4]. To improve the previous understandings, Kim et al. [5] performed an experimental investigation and proposed a model based on the volume averaging method for predicting the pressure drop and the thermal resistance of both configurations. They concluded that when the dimensionless length of heat sinks is large and dimensionless pumping power is small, optimized pin-fin heat sinks have lower thermal resistances than optimized plate-fin

* Corresponding author.
E-mail address: H.Towsyfyan@soton.ac.uk (H. Towsyfyan).

https://doi.org/10.1016/j.csite.2018.100388
Received 8 October 2018; Received in revised form 26 December 2018; Accepted 30 December 2018
Available online 03 January 2019

heat sinks. However, the optimized plate-fin heat sinks possess smaller thermal resistances when dimensionless pumping power is large and the dimensionless length of heat sinks is small.

Not limited to the common type of heat sinks, a considerable body of research has been concentrated to investigate the enhancement of heat transfer rate through applying other type of fins. This mainly includes hollow rectangular profile fins [6], rectangular perforation fins [7,8] square and circular perforation fins [9–11], triangular perforation fins [12], inclined plate fins [13,14] and flared fins [2].

Beside demonstrating the effect of fin shape on the enhancement of heat transfer rate, research has been reported in the literature showing that other parameters may also have significant influence on the thermal performance of heat sinks. For instance, some of the above studies looked at the efficiency of different fin arrays [8,11] as well as fin size and spacing [8,13,15]. In Ref [15], it has also been reported that the fin thickness has more influence on thermal performance of heat sinks compared to the number of fins. In another paper, Li et al. [16] carried out a numerical and experimental study to examine the effect of several parameters including width and height of fins, distance of impinging and jet velocity on the thermal performance of plate-fin heat sinks. They reported that these parameters have considerable effect on the thermal characteristics of heat sinks as well.

To investigate the possibility of further enhance in the heat transfer efficiency of the plate-fin heat sinks, kok-cheong wong and sanjiv indran [17] studied the effect of fillet profile on the thermal performance of heat sinks. They reported that adding a fillet profile at the bottom of plate-fin heat sinks improves their overall thermal performance by approximately 13%.

Above understandings reveal there is a good correlation between the design parameters of fins and thermal performance of heat sinks. For the remainder of this paper, plate-fin heat sinks with fillet profile are considered and compared with plate-fin heat sinks without fillet profile (as a part of numerical analysis that will be carried put in Section 4.2) since they offer simple design, easy fabrication and implementation. Pin-fin heat sinks, however, provide higher heat transfer coefficient that comes at the expense of higher production cost.

Therefore, the efficiency of plate-fin heat sinks can be improved realistically by establishing an effective flow direction. Many researchers have considered analytical solutions for the heat transfer enhancement of plate-fin heat sinks in both parallel and impinging flow. The former has been studied based on the Nusselt number [18], optimisation of entropy generation [19] and a pressure drop model [20]. In case of plate-fin heat sinks by applying impinging flow, Biber [21] developed numerically obtained correlations for pressure loss coefficient and total heat transfer in a variable-length channel that covers a wide range of practical plate-fin heat sinks. Later on, Saini and Webb [22] validated Biber model by experiments and made some modifications and improvements. In another work, Duan and Muzychka [23] developed a simple semi-empirical model for predicting the pressure drop and the heat transfer coefficient of air-cooled plate-fin heat sinks.

However, to the best knowledge of the authors, the development of a CFD based model that can demonstrate the effect of flow direction on the plate-heat sinks with fillet profile, as a primary phase to increase the performance of conventional heat sinks in electronic devices, has not yet been reported. This is of high importance in engineering applications to develop effective cooling technologies as the extra heat may degrade the function of the electronic devices.

This paper attempts to fill this gap and presents a numerical analysis to compare thermal performance of plate-fin heat sinks with fillet profile subject to parallel flow and those without fillet profile subject to impinging. The impact of this research work can be better understood by considering the limitations of the fan place in electronic equipment industry (e.g. the lack of available space on the side and top surfaces of the electronic box). With the help of this study, it is possible to improve the thermal performance of plate-fin heat sinks (as their lower production cost comes at the expense of lower heat transfer rate) based on the flow direction and fillet profile.

2. Numerical computation

In this section, the investigation develops a CFD model to analyze the convective heat transfer in plate-fin heat sinks. There are three main steps in CFD analysis: (a) pre-processing, (b) solver execution and (c) post-processing. The former step includes creating the geometry of the desired model as well as the mesh generation, whilst as expected, the results are presented in the last step. Boundary conditions are fed into the model in the solver execution (middle) stage.

2.1. Geometry

In this paper, two geometries i.e. plate-fin heat sinks without fillet profile and plate-fin heat sinks with fillet profile are investigated as shown in Fig. 1(a) and (b) respectively. For the plate-fin heat sink with fillet profile, the optimum radius of fillet profile equal to 1.5 mm is considered for the remainder of paper as detailed in Ref. [17].

The base dimension measures 40 mm × 39.7 mm, with thickness of 5 mm. The channel width and thickness of fin is assumed to be constant across the length of the base and measures 3.3 mm and 1 mm respectively as shown in Fig. 1(a). Moreover, the fin height in Fig. 1(a) and (b) are different and measures 25 mm and 28.6 mm respectively. The difference is due to the compensation for the volume of solid material that removed from the base to generate fillet, as detailed in appendix A.

For the remainder of paper, the plate-fin heat sink subject to impinging flow, in which air impinges on the heat sink along the y-axis and then flows parallel to x-axis, refers to as the conventional design. Proposed design refers to as a plate-fin heat sink subject to parallel flow so that the air flows into the heat sink along the x-axis, Fig. 1.

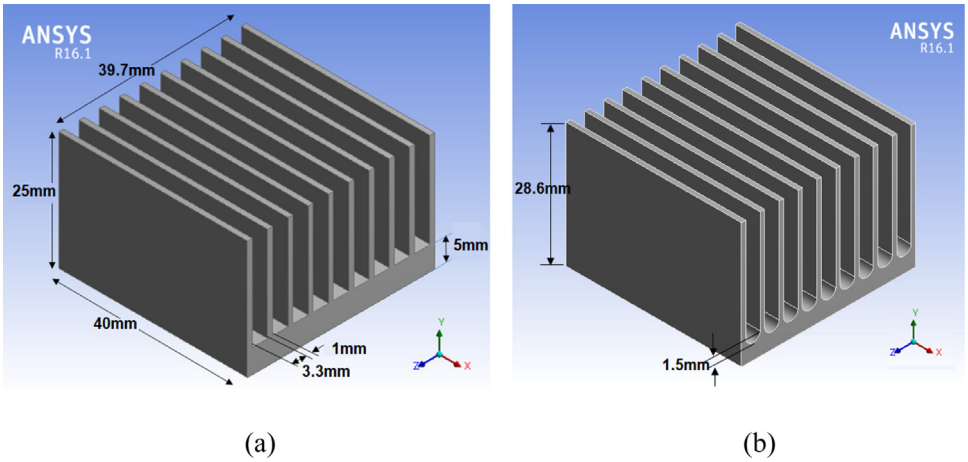

Fig. 1. The geometrical model (a) Conventional design and (b) Proposed design.

2.2. Mesh generation

In this paper, ANSYS FLUENT R16.0 is used to construct the computational grid as well as to discretize and to solve the governing equations as detailed in Section 2.4. To ensure the accuracy of the simulations, the mesh needs to be generated with care in terms of computational time. Moreover, to ensure the mesh independency of numerical results, grid independency test is needed to be carried out.

Table 1 illustrates numerical results for the base temperature with different mesh configurations. Two cases are considered, i.e. plate-fin heat sinks with and without fillet profile. As it is evident, a significant increase in the number of grid elements does not lead to a notable change in the results, i.e. base temperature. Based on Table 1 the difference between the results, either for plate-fin heat sinks without fillet profile or plate-fin heat sinks with fillet profile, remains negligible.

Therefore, to reduce the computation time, the mesh with lower elements will be used for the remainder of the paper. The exploratory experiments in present work have shown that the mesh size with 721704 elements meets the requirements of accuracy and computation time as shown in Fig. 2. Moreover, a good agreement is evident between the numerical results and experimental data presented in [5], as detailed in Section 4.1, that proves the choice of number of element in numerical side (CFD). For the pressure-velocity coupling, the SIMPLE (Semi Implicit Method for Pressure Linked Equation) algorithm is applied.

2.3. Boundary conditions

In this research, boundary conditions are considered similar to the work published by Kim et al. [5] where a constant heat flux of 18750W/m^2 along with a variable value of inlet air flow (i.e. 0.00092, 0.00218, 0.0033 and 0.00433 kg/s) has been applied. In their experimental work, as shown schematically in Fig. 3, the plate-fin heat sink (made of aluminium alloy 6061) is positioned in the wind tunnel (made of acrylic) and air impinges into the tunnel from a pressure tank through a mass flow meter. Electrical heaters warm the heat sink up and the temperature distribution at the base of the heat sink at different flow rates is measured by thermocouples. In order to measure the pressure difference between the inlet and the outlet of the heat sink, a pressure tap is mounted on the wind tunnel wall that is connected to a manometer. Interested readers are encouraged to see Ref. [5] for more details on experimental set up, measurement systems and test procedures.

2.4. Numerical modeling

Navier-Stokes (N-S), energy and continuity equations are solved numerically to simulate the convective heat transfer process, under some simplification and presumptions as followings:

Table 1
Results of the mesh independency tests.

Design of heat sink profile	Number of elements(million)	Base temperature (°C)	Difference in temperature (%)
without fillet	0.72	80.871	0.106
	1.5	80.957	
with fillet	2.8	78.85	0.16
	5.5	78.98	

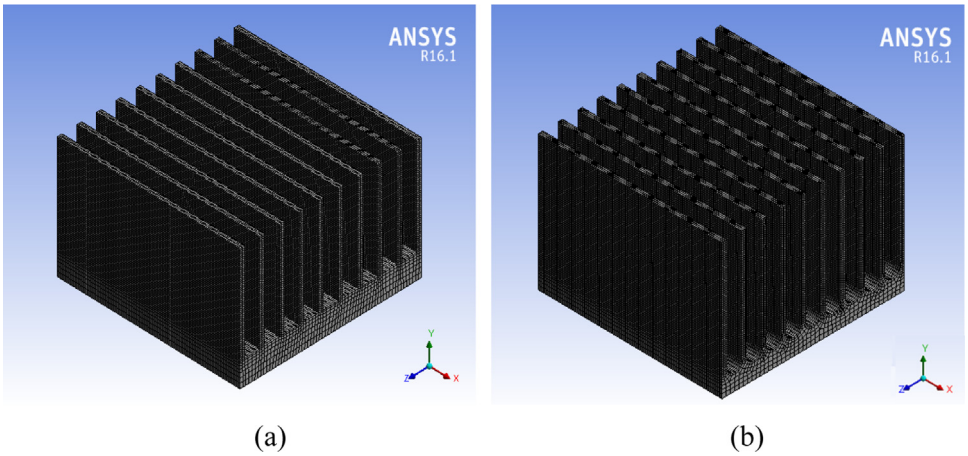

Fig. 2. The mesh of domain (a) Conventional design and (b) Proposed design.

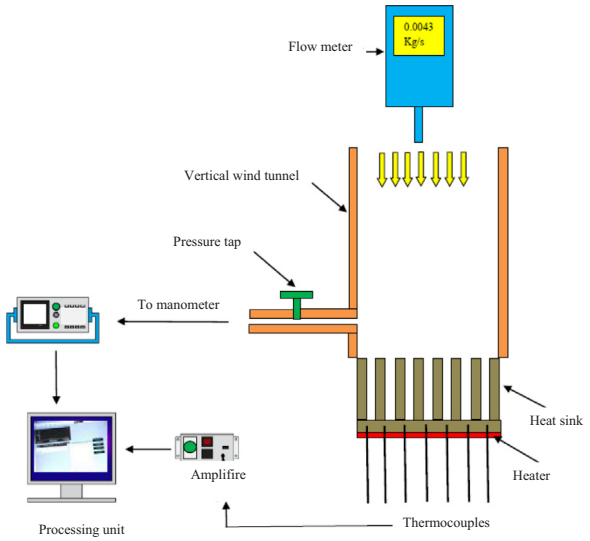

Fig. 3. Schematic illustration of the experimental apparatus applied in Ref [5].

1. The air flow is steady, turbulent and incompressible flow.
2. Three-dimension fluid-solid conjugate.
3. All properties of coolant air depend on its mean temperature.

The N-S equations across the x, y and z directions are given as followings:

$$\nabla(\rho\vec{U}u) = -\frac{\partial p}{\partial x} + \frac{\partial \tau_{xx}}{\partial x} + \frac{\partial \tau_{yx}}{\partial y} + \frac{\partial \tau_{zx}}{\partial z}$$

$$\nabla(\rho\vec{U}v) = -\frac{\partial p}{\partial y} + \frac{\partial \tau_{xy}}{\partial x} + \frac{\partial \tau_{yy}}{\partial y} + \frac{\partial \tau_{zy}}{\partial z} \quad (1)$$

$$\nabla(\rho\vec{U}w) = -\frac{\partial p}{\partial z} + \frac{\partial \tau_{xz}}{\partial x} + \frac{\partial \tau_{yz}}{\partial y} + \frac{\partial \tau_{zz}}{\partial z}$$

where ρ is the density of fluid, (u, v and w) are velocity components in three directions, $\vec{U}$ is the velocity, τ is the viscous stress tensor and p is pressure.

The energy equation is given by:

$$\nabla(\rho h\vec{U}) = -p\nabla\vec{U} + \nabla(k\nabla T) + \phi + s_h \quad (2)$$

where h is the aggregate enthalpy, ϕ is the dissipation term, k is thermal conductivity, T is temperature and s_h is the source term.

Finally, the continuity equation is given by:

$$\nabla(\rho\vec{U}) = 0 \tag{3}$$

The energy and momentum conservation equations are discretized in ANSYS FLUENT R16.0 by a second-order upwind interpolation scheme that is utilized to calculate cell-face pressure.

3. Calculation procedure

The average Nusselt number, $\bar{Nu}$, estimates the performance of a plate-fin heat sink and can be computed based on the following equation:

$$\bar{Nu} = \frac{\bar{h}D_h}{K_a} \tag{4}$$

where D_h is the hydraulic diameter of the inlet, $\bar{h}$ is the mean heat transfer coefficient and K_a is the thermal conductivity of coolant fluid (air). The latter is tabulated based on the mean temperature, T_m, that is given by Eq. (5) as following:

$$T_m = \frac{(T_{avr} + T_b)}{2} \tag{5}$$

where T_b is base of fin temperature and T_{avr} represents average air temperature given by Eq.(6):

$$T_{avr} = \frac{(T_{out} + T_{in})_a}{2} \tag{6}$$

where T_{out} and T_{in} are outlet and inlet temperature of air respectively. In Eq. (4) the mean heat transfer coefficient, $\bar{h}$, is prescribed by:

$$\bar{h} = \frac{Q}{A_T(T_b - T_m)} \tag{7}$$

where Q is the heat transfer rate to the cool medium (air) by convection, A_T is the total area that is subjected to the cooling fluid and T_m is the mean temperature of air.

In Eq. (7), the heat transfer rate, Q, and total cooling area, A_T, can be expressed by Eqs. (8) and (9) respectively [11]:

$$Q = \dot{m}_a C_{Pa}(T_{out} - T_{in}) \tag{8}$$

where $\dot{m}_a$ and C_{Pa} are the mass flow rate and the specific heat of air respectively.

$$A_T = WL+2N_f H[L + t]+2B[L + W] \tag{9}$$

where W and L are the width and length of heat sink respectively, N_f represents the number of fins, H, t and B are the height, thickness of fins and base height respectively.

Substituting Eqs. (8) and (9) into Eq. (7), the mean heat transfer coefficient, $\bar{h}$, can be calculated by Eq.(9):

$$\bar{h} = \frac{\dot{m}_a C_{Pa}(T_{out} - T_{in})}{(WL+2N_f H[L + t]+2B[L + W])(T_b - T_m)} \tag{10}$$

Substituting Eq. (10) into Eq. (4) gives the average Nusselt number as following:

$$\bar{Nu} = \frac{\dot{m}_a C_{Pa}(T_{out} - T_{in})}{(WL+2N_f H[L + t]+2B[L + W])(T_b - T_m)}\frac{D_h}{K_a} \tag{11}$$

The pressure drop, ΔP, between the inlet and outlet along with the thermal performance, R_{th}, of plate-fin heat sinks is particularly important in this paper and will be used in Section 4 to interpret the results. These parameters can be evaluated based on Eqs. (12) and (13) respectively:

$$\Delta P = P_{in} - P_{out} \tag{12}$$

where, P_{in}andP_{out} are inlet and outlet pressure respectively.

$$R_{th} = \frac{1}{\bar{h}A_T} \tag{13}$$

4. Result and discussion

4.1. Validation of numerical computations

To be fair in comparison, the boundary conditions, geometry of plate-fin heat sinks (without profile) and direction of flow (impinging flow) is considered exactly similar to the experimental study carried out in Ref [5]. On this basis, thermal resistance and pressure drop of air at different mass flow rates are compared as illustrated in Figs. 4 and 5 respectively.

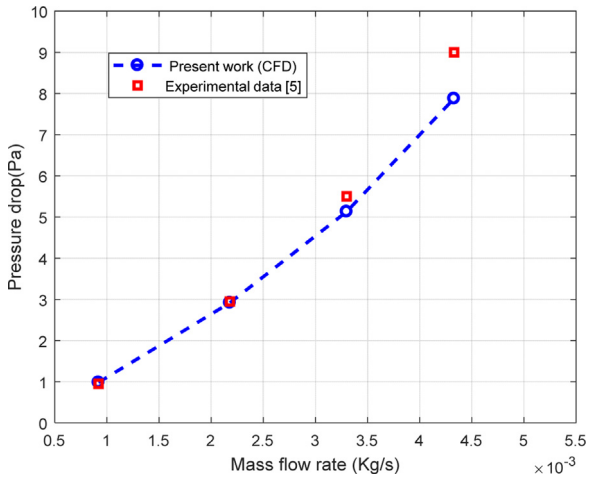

Fig. 4. Validation of CFD results for pressure drop at different mass flow rates.

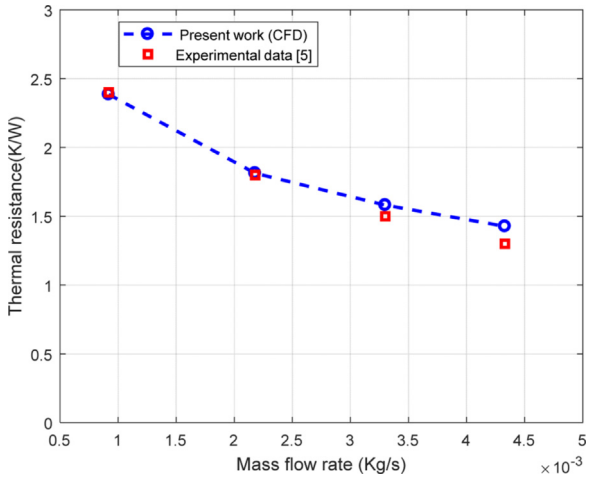

Fig. 5. Validation of CFD results for thermal resistance at different mass flow rates.

As it is evident, good agreement is observed between the results of numerical solution (CFD) and the experimental work of Kim et al. [5]. The maximum discrepancy is 8.8% and 12.4% for thermal resistance and pressure drop respectively. A plausible explanation for the difference could be, perhaps, due to the thermal losses and measurement errors.

Therefore, it can be concluded that the developed numerical approach is accurate enough and can be effectively applied to investigate the effect of flow direction and fillet profile on the thermal performance of heat sinks, as detailed in Section 4.2.

4.2. The results of numerical study

Having validated the numerical computations with an experimental study, this section aims to clearly identify the impact of the fillet profile and direction of flow on the efficiency of plate-fin heat sinks. To be robust in comparison, three sets of simulations will be detailed. First, the effect of fillet profile in impinging flow is investigated. This is next followed by a numerical study on the effect of flow direction on plate-fin heat sinks with fillet profile. The section concludes with a focus on the comparison of proposed and conventional designs based on numerical simulations.

4.2.1. The effect of fillet profile

The effect of fillet profile on thermal efficiency of an air-impinged plate fin heat sink has already been investigated numerically (and validated against experimental data) in Ref [17].

To improve previous understandings and to distinct the contribution of adding a fillet profile to the overall thermal enhancement of proposed design, plate-fin heat sinks with and without profile are compared in this section. Fig. 6 presents the temperature contour of the plate-fin heat sink subject to impinging flow for two different configurations, i.e. with fillet profile and without it. As it is expected in plate-fin heat sinks with fillet profile, due to the increase in heat transfer area, more amount of heat is removed from the

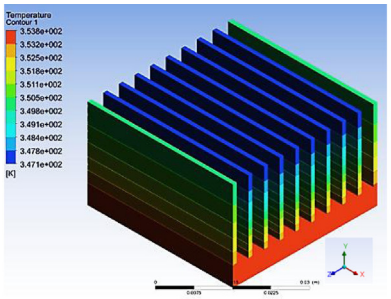

Without fillet profile at flow rate of 0.00092kg/s

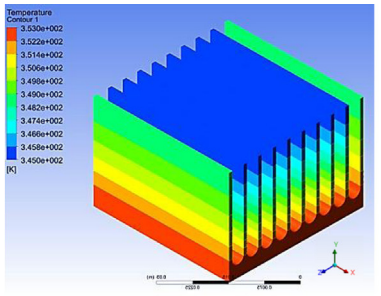

With fillet profile at flow rate of 0.00092kg/s

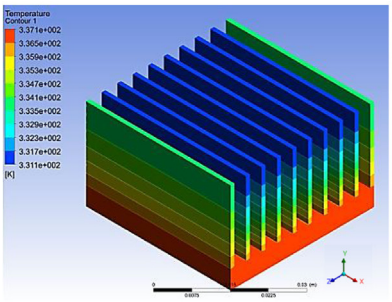

Without fillet profile at flow rate of 0.00218Kg/s

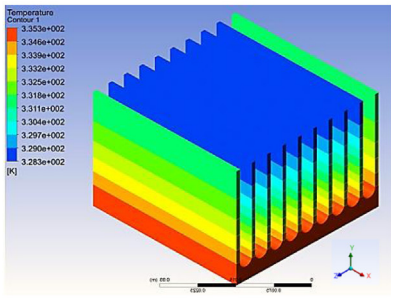

With fillet profile at flow rate of 0.00218Kg/s

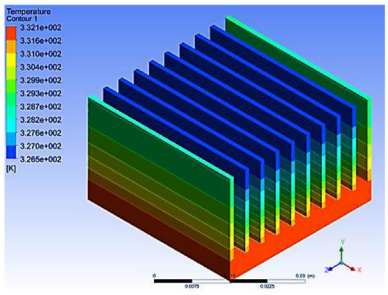

Without fillet profile at flow rate of 0.0033Kg/s

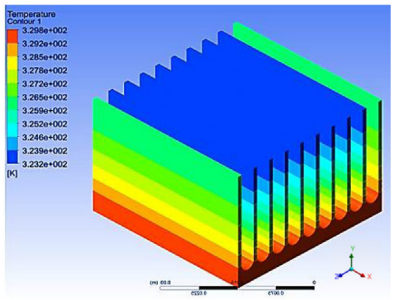

With fillet profile at flow rate of 0.0033Kg/s

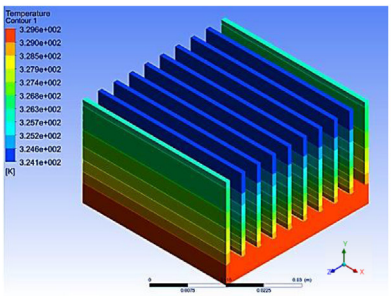

Without fillet profile at flow rate of 0.00433Kg/s

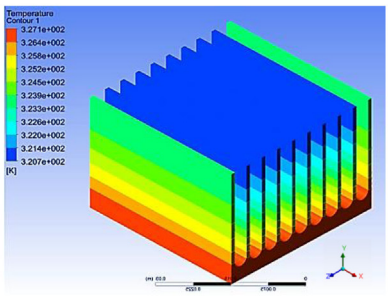

With fillet profile at flow rate of 0.00433Kg/s

Fig. 6. Contour temperature of heat sink with and without fillet profile at various mass flow rates of air.

hot region. Therefore, the base temperature for plate-fin heat sinks with fillet profile is less than those without fillet profile. Moreover, the heat distribution is altered by the fillet profile that proves the superior thermal performance of this configuration.

To investigate the effect of adding a fillet profile on the efficiency of plate-fin heat sinks subject to impinging flow, the variation of

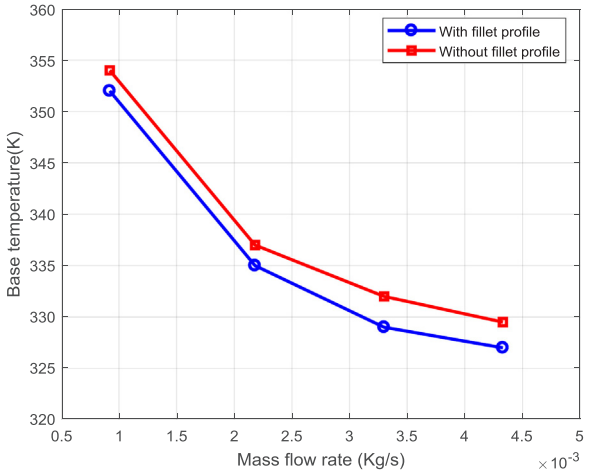

Fig. 7. Compression of the base temperature in plate-fin heat sinks with and without fillet profile subject to impinging flow at different flow rates.

heat-sink's base temperature along with thermal resistance of both configurations (i.e. with and without fillet profile) is compared at various values of the air mass flow rate in Figs. 7 and 8 respectively.

As it is evident in figures, the base temperature and thermal resistance decrease by the mass flow rate increase in both configurations. However, the base temperature and thermal resistance of a heat sink with fillet profile are approximately 3.78% and 5.18% lower compared to a plate-fin heat sink without fillet profile at different mass flow rates that is in good agreement with previous works [17].

4.2.2. The effect of flow direction

The effect of flow direction on the thermal performance of conventional plate-fin heat sinks without fillet profile has already been studied in Refs [19–23]. This section aims to study the effect of flow direction in plate-fin heat sinks with fillet profile and hence, provide a better understanding of its contribution to the overall thermal enhancement of proposed design (i.e. plate-fin heat sink with fillet profile subject to parallel flow) that will be detailed in next section.

As it is evident in Fig. 9, for both configurations, the area that is directly blown by the fan remains cooler for all flow rates. In impinging flow, however, the hot region occupies the base of the heat sink whilst the cold region settled in the top of the fin indicating the lower thermal efficiency of this configuration.

In parallel flow the temperature contours show more effective thermal distribution between the base and upper region of the heat sink that may lead to a notable thermal efficiency enhancement.

To study the effect of flow direction on the thermal performance of plate-fin heat sinks, the variation of heat-sink's base temperature along with thermal resistance of both configurations (i.e. impinging flow and parallel flow) is compared at various values of the air mass flow rate in Figs. 10 and 11 respectively. As it is evident, the base temperature and thermal resistance of a plate-fin heat sink with fillet profile subject to parallel flow are approximately 3.85% and 5.29% lower at different mass flow rates compared to a

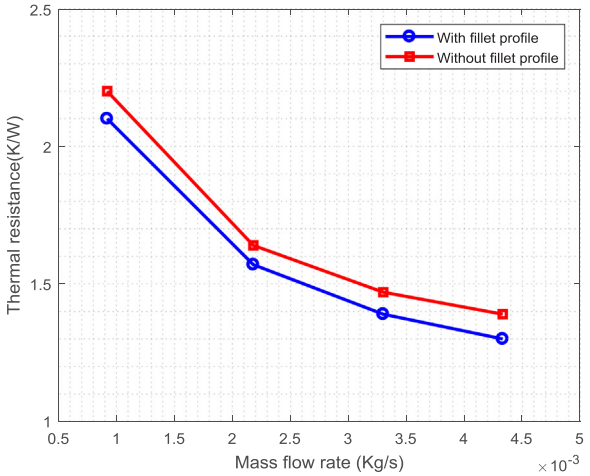

Fig. 8. Compression of the base thermal resistance in plate-fin heat sinks with and without fillet profile subject to impinging flow at different flow rates.

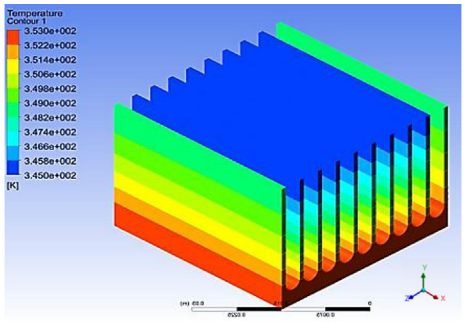

Impinging flow at flow rate of 0.00092kg/s

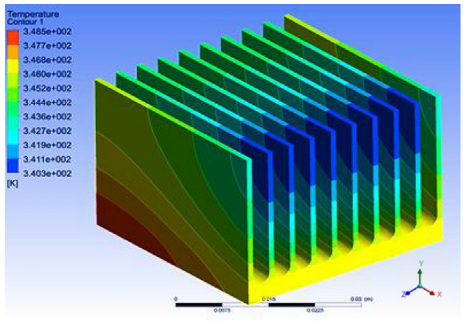

Parallel flow at flow rate of 0.00092kg/s

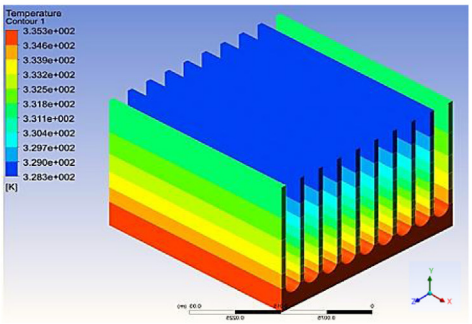

Impinging flow at flow rate of 0.00218Kg/s

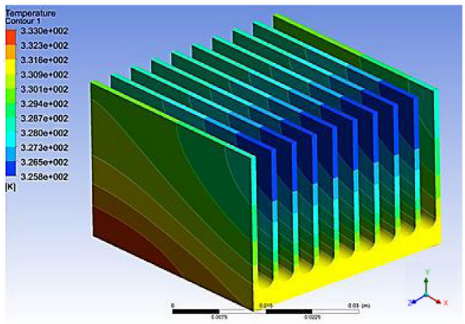

Parallel flow at flow rate of 0.00218Kg/s

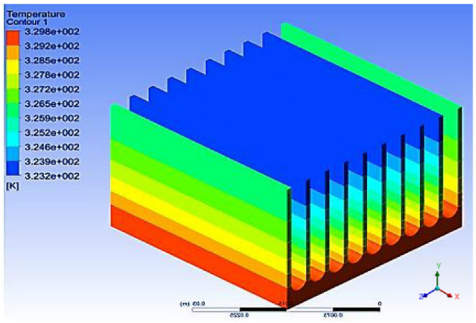

Impinging flow at flow rate of 0.0033Kg/s

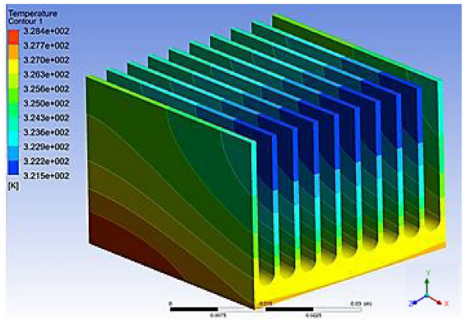

Parallel flow at flow rate of 0.0033Kg/s

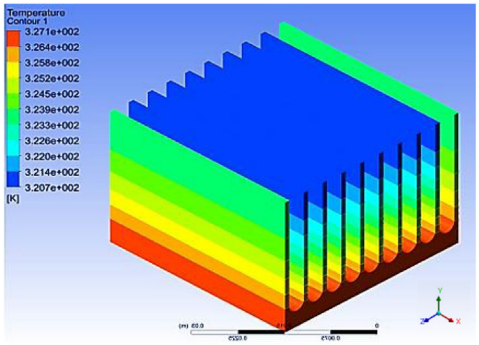

Impinging flow at flow rate of 0.00433Kg/s

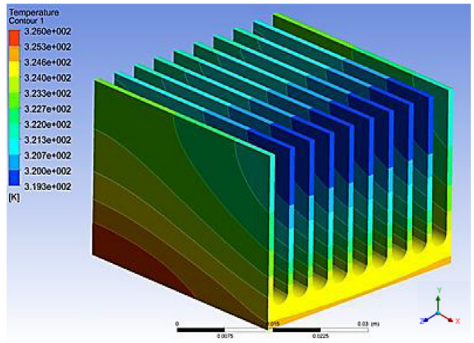

Parallel flow at flow rate of 0.00433Kg/s

Fig. 9. Contour temperature of heat sinks subject to different flow direction of air.

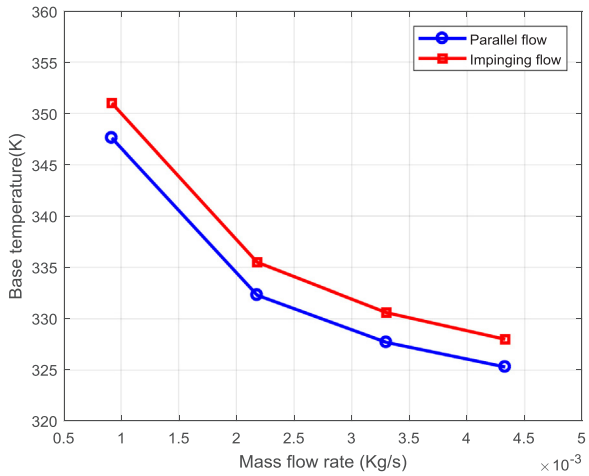

Fig. 10. Compression of the base temperature in plate-fin heat sinks with fillet profile subject to different flow direction at various flow rates.

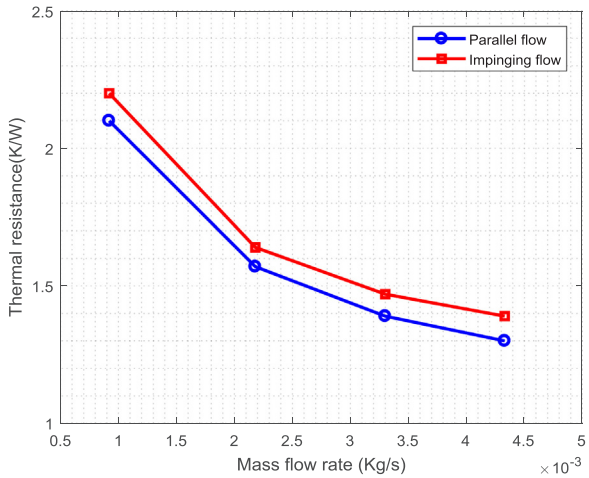

Fig. 11. Compression of the base thermal resistance in plate-fin heat sinks with fillet profile subject to different flow direction at various flow rates.

plate-fin heat sink with fillet profile subject to impinging flow.

4.2.3. Proposed design vs. conventional design

Having investigated the effect of fillet profile and flow direction on thermal performance of plate-fin heat sinks, the conventional design (plate-fin heat sink without fillet profile subject to impinging flow) is compared with the proposed design (plate-fin heat sink with fillet profile subject to parallel flow) in terms of temperature difference and thermal resistance.

Fig. 12 shows the temperature contour of the plate-fin heat sink for both proposed and conventional designs at various mass flow rates of air. As it is evident in conventional design, the hot region occupies the base of the heat sink whilst the cold region settled in the top of the fin indicating the lower thermal efficiency of this design. However, by creating a fillet, the temperature contours show an effective thermal distribution between the base and upper region of the heat sink that leads to a notable thermal efficiency enhancement as has been discussed in Section 4.2.1. In addition, the heat distribution is altered by the fillet profile and hence the convection is smoothened near the bottom of the plate fin.

Moreover, since in the proposed approach the fan is located closer to the base of heat sink, therefore, more amount of heat is removed from the hot region. Hence, the base region remains cooler for the proposed design. As it has been detailed in Section 4.2.2, for both configurations, the area that is directly blown by the fan (i.e. top region in conventional design and side region in proposed design) remains cooler for all flow rates. However, the coldest area (dark blue region) is significantly lower for proposed design indicating the superior thermal efficiency of this model over the conventional design.

To get insight into the efficiency of proposed design, the variation of heat-sink's base temperature of conventional model is compared with the proposed design at various values of the air mass flow rate in Fig. 13.

As it is evident, the base temperature of heat sink is approximately 7.5% lower for the proposed approach at different mass flow rates that shows a notable improvement in design. This could be the effect of adding a fillet profile along with flow direction as has

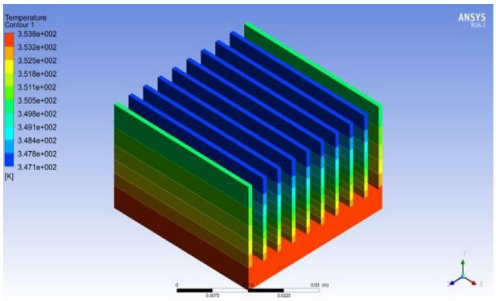

Conventional design at flow rate of 0.00092kg/s

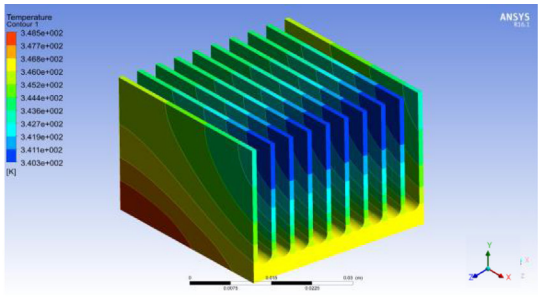

Proposed design at flow rate of 0.00092 Kg/s

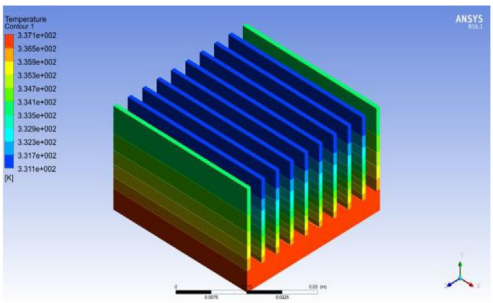

Conventional design at flow rate of 0.00218Kg/s

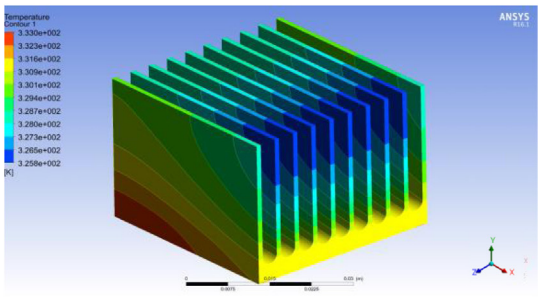

Proposed design at flow rate of 0.00218Kg/s

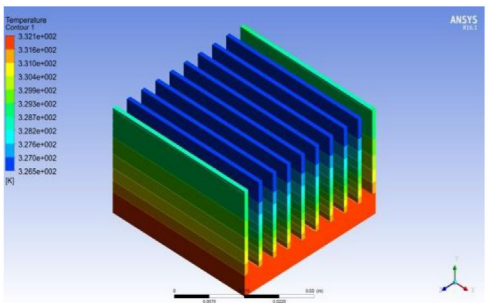

Conventional design at flow rate of 0.0033Kg/s

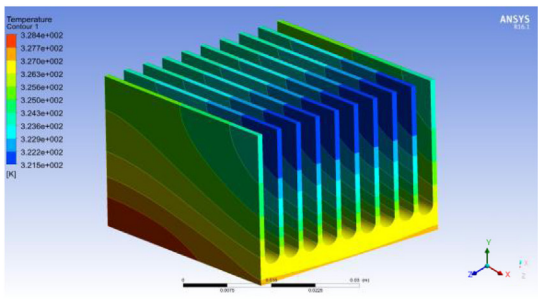

Proposed design at flow rate of 0.0033Kg/s

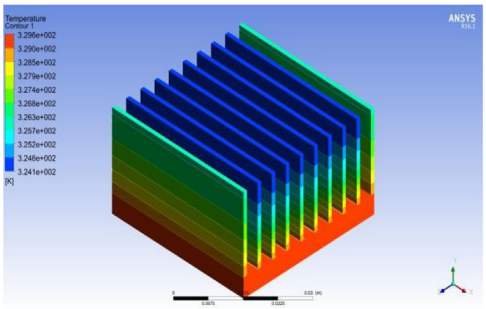

Conventional design at flow rate of 0.00433Kg/s

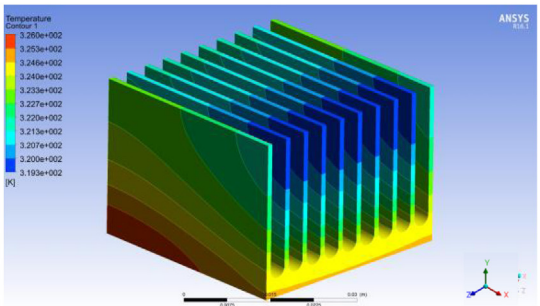

Proposed design at flow rate of 0.00433 Kg/s

Fig. 12. Contour temperature of heat sink for conventional and proposed design at various mass flow rate of air.

already been discussed in Sections 4.2.1 and 4.2.2.

In Fig. 14, variation of thermal resistance for the conventional design is compared with the proposed approach at various values of the air mass flow rate. A notable difference (approximately 18%) is evident between thermal resistance of the proposed design and

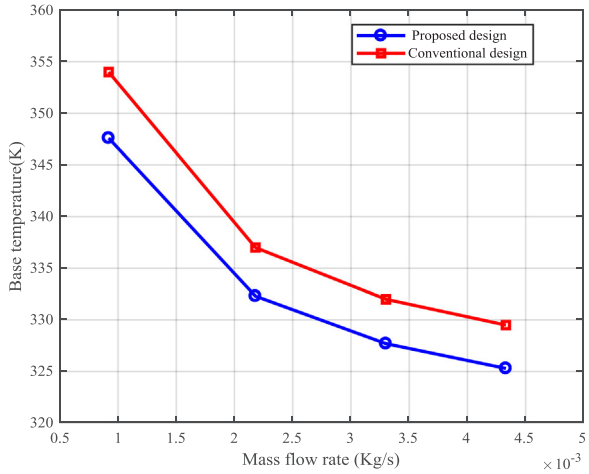

Fig. 13. Compression of the base temperature in plate-fin heat for the conventional design and proposed approach at different flow rates.

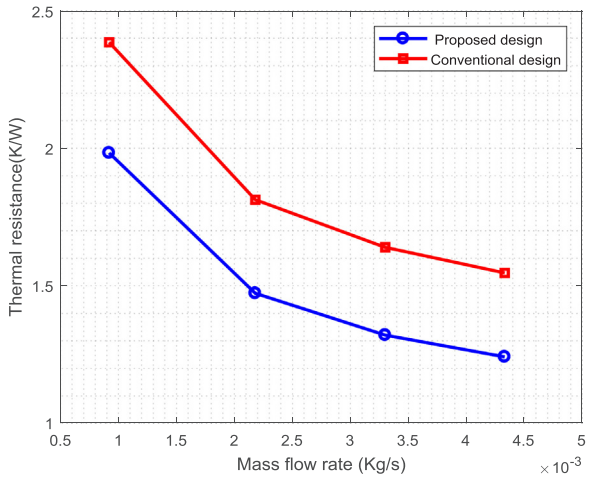

Fig. 14. Compression of the base thermal resistance in plate-fin heat sinks for the conventional design and proposed approach at different flow rates.

conventional design that may prove the efficiency of proposed approach. A plausible explanation for such improvement in proposed approach is that, in addition to the effect of fillet profile and flow direction that have been discussed in previous sections, the average heat transfer coefficient goes up due to the temperature gradient increase between the base of heat sink and the airflow. Therefore, the thermal resistance is lower as it is inversely proportional to the surface area and coefficient of heat transfer, Eq. (13).

5. Conclusions

Thermal performance of plate-fin heat sinks with fillet profile subject to parallel flow (proposed design) and those without fillet profile subject to impinging (so called conventional design in the paper) has been compared. To achieve this, a CFD model for plate-fin heat sinks without fillet profile subject to impinging has been developed and validated with an experimental study from the literature. The obtained results demonstrated that the maximum difference between experimental data and numerical results were 12.4% and 8.8% for pressure drop and the thermal resistance respectively under same conditions. This proves the accuracy of the numerical analysis that has been developed in this study.

In particular, three sets of simulations have been discussed, i.e. the effect of fillet profile on plate-fin heat sinks subject to impinging flow, the effect of flow direction on plate-fin heat sinks with fillet profile and the comparison of the proposed design and conventional design.

The study has shown that adding a fillet profile and changing the flow direction (from impinging to the parallel flow) have a notable effect on thermal performance of plate-fin heat sinks. Although, this was beyond the scope of present paper to demonstrate which one has superior effect, the primary results have shown that both parameters have approximately same effect on base temperature and thermal resistance of heat sinks.

Furthermore, the numerical results of comparison between proposed design and conventional design shown that the base

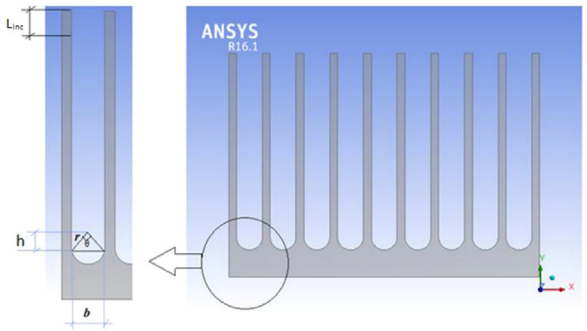

The geometry of fillet .1-A .gFi

Fig. A-1. The geometry of fillet.

temperature of heat sink in proposed design decreases by 7.5% compared to the conventional model. Moreover, the thermal resistance for proposed design is 18% lower in comparison with the conventional design. Therefore, a notable improvement in the thermal performance of the heat sink was demonstrated that might help to develop more advanced cooling technologies for electronic equipment industry.

Acknowledgement

The authors wish to express their deep thanks and gratitude to the support provided by (Mustansiriyah University) to accomplish the present work.

Appendix A. Calculation of the fin height for fillet profile

See Fig. A-1

The value of cutted material from the based and added material to the top has to be equal

$$V_{cut} = V_{add} \tag{A.1}$$

This means that:

$$\left[\left(\left(\frac{\theta}{360}\right) \times \pi r^2 \right) - 0.5b \times h)\right] \times 40 \times n = L_{inc} \times t \times 40 \times N \tag{A.2}$$

where, n is number of fillets (9 in present research), N is number of fins (10 in present research), b is pitch (3.3 mm in present research), t is thickness of fin (1 mm in present research), h is high of triangle (achieved by $\sqrt{r^2 - (0.5b)^2}$)

From the equation above the increase in length of fin (L_{inc}) can be calculated.

Appendix B. Nomenclature and subscripts

NOMENCLATURE		
A	Area of heat transfer,	m^2
B	Base height	m
b	Pitch	m
C_P	Specific heat	W/ kg. °C
D_h	Hydraulic diameter,	m
H	Height of fin	m
h	High of triangle	m
$\bar{h}$	Average heat transfer coefficient,	W/ m^2 °C
k	Thermal conductivity,	W/ m °C
L	Length of heat sink	m

L_{inc}	Increase in length of fin	m
$\dot{m}$	Mass flow rate,	Kg/s
N_f	Number of fins	
n	Number of fillet	
Q	Rate of heat transfer	w
$\bar{Nu}$	Average Nusselt number,	
R_{th}	Thermal resistance,	°K/W
P	Pressure,	pas
V	Volume	m^3
T	Temperature,	°C
t	Thickness of fin	m
W	Width of heat sink	m

SUBSCRIPTS	
a	Air
add	Adding
avr	Average
b	Base
cut	Cutting
f	Film
in	Inlet
inc	Increase
m	Mean
out	Outlet
T	Total

References

[1] A. Bar-Cohen, Thermal management of electric components with dielectric liquids, in: J.R. Lloyd, Y. Kurosaki (Eds.), Proceedings of ASME/JSME Thermal Engineering Joint Conference, vol. 2, 1996, pp. 15–39.
[2] F. Forghan, D. Goldthwaite, M. Ulinski, M. Metghalchi, Experimental and theoretical investigation of thermal performance of heat sinks, ISME (2001).
[3] Y. Kondo, H. Matsuhima, Study of impingement cooling of heat sinks for LSI packages with longiudinal fins, Heat. Transf. Jpn. Res. 25 (1996) 537–553.
[4] H.-Y. Li, S.-M. Chao, G.-L. Tsai, Thermal performance measurement of heat sinks with confined jet by infrared thermography, Int. J. Heat. Mass Transf. 48 (2005) 5386–5394.
[5] D.-K. Kim, S.J. Kim, J.-K. Bae, Comparison of thermal performances of plate-fin and pin-fin heat sinks subject to an impinging flow, Int. J. Heat. Mass Transf. 52 (2009) 3510–3517.
[6] U. Akyol, K. Bilen, Heat transfer and thermal performance analysis of a surface with hollow rectangular fins, Appl. Therm. Eng. 26 (2006) 209–216.
[7] A.H. AIEssa, Ayman M. Maqableh, Shatha Ammourah, Enhancement of natural convection heat transfer from a fin by rectangular perforations with aspect ratio of two, Int. J. Phys. Sci. 4 (2009) 540–547.
[8] Guei-Jang Huang, Shwin-Chung Wong, Chun-Pei Lin, Enhancement of natural convection heat transfer from horizontal rectangular fin arrays with perforations in fin base, Int. J. Therm. Sci. 84 (2014) 164–174.
[9] N. Souidi, A. Bontemps, Countercurrent gas- liquid flow in plate –fin heat exchangers with plain and perforated fins, Int. J. Heat. Fluid Flow. 22 (2001) 450–459.
[10] A.H.M. AIEssa, Augmentation of fin natural convection heat dissipation by square perforations, J. Mech. Eng. Autom. 2 (2012) 1–5.
[11] Kavita H. Dhanawade, Vivek K. Sunnapwar, Hanamant S. Dhanawade, Thermal analysis of square and circular perforated fin arrays by forced onvection, Int. J. Curr. Eng. Technol. 2 (2014) 109–114.
[12] A.H. AIEssa, Mohammed Q. Al-Odat, Enhancement of natural convection heat transfer from a fin by triangular perforations of bases parallel and toward its base, Arbian J. Sci. Eng. 34 (2B) (2009) 531–544.
[13] I. Tari, M. Mehrtash, Natural convection heat transfer from horizontal and slightly inclined plate-fin heat sinks, Appl. Therm. Eng. 61 (2) (2013) 728–736.
[14] I. Tari, M. Mehrtash, Natural convection heat transfer from inclined plate-fin heat sinks, Int. J. Heat. Mass Transf. 56 (1–2) (2013) 574–593.
[15] Mohamed H.A. Elnaggar, heat transfer enhancement by heat sink fin arrangement in electronic cooling, J. Multidiscip. Eng. Sci. Technol. (JMEST) 2 (3) (2015) 457–460.
[16] H.-Y. Li, K.-Y. Chen, M.-H. Chiang, Thermal-fluid characteristics of plate-fin heat sinks cooled by impingement jet, Energy Convers. Manag. 50 (2009) 2738–2746.
[17] Kok-Cheong Wong, Sanjiv Indran, Impingement heat transfer of a plate fin heat sink with fillet profile, Int. J. Heat. Mass Transf. 56 (2013) 1–9.
[18] P. Teertstra, M. Yovanovich, J.R. Culham, T. Lemczyk, Analytical forced convection modeling of plate fin heat sinks, in: Proceedings of the 15th IEEE Semi-Therm Symposium, iugguyfgu, 1999, pp. 34–41.
[19] J.R. Culham, Y.S. Muzychka, Optimization of plate fin heat sinks using entropy generation minimization, IEEE Trans. Compon. Packag. Technol. 24 (2001) 159–165.
[20] D. Copeland, Optimization of parallel plate heat sinks for forced convection, in: Proceedings of the 16th IEEE Semi-therm Symposium, San Jose, CA, 2000, pp. 266– 272.
[21] C.R. Biber, Pressure drop and heat transfer in an isothermal channel with impinging flow, IEEE Trans. Compon. Packag. Manuf. Technol. A 20 (1997) 458–462.
[22] M. Saini, R.L. Webb, Validation of models for air cooled plane fin heat sinks used in computer cooling, in: Proceedings of the Eighth Intersociety Conference on Thermal and Thermomechanical Phenomena in Electronic Systems, San Diego, CA, 2002, pp. 243–250.
[23] Z. Duan, Y.S. Muzychka, Pressure drop of impingement air cooled plate fin heat sinks, Trans. ASME 129 (2007) 190–194.